J Radioanal Nucl Chem (2009) 282:349–354
DOI 10.1007/s10967-009-0328-8

Reductive immobilization of ^{79}Se by iron canister under simulated repository environment

D. Cui · A. Puranen · J. Devoy · A. Scheidegger · O. X. Leupin · P. Wersin · R. Gens · K. Spahiu

Received: 15 July 2009 / Published online: 12 August 2009
© Akadémiai Kiadó, Budapest, Hungary 2009

Abstract To understand the fate of ^{79}Se in a repository-like environment, the interactions between iron canister surface with dissolved selenite (SeO_3^{2-}) and selenate (SeO_4^{2-}) in anaerobic solutions have been investigated. Se(IV) immobilization on iron surface was observed to be about 100 times faster than that of Se(VI) at same conditions. An iron surface coated with a $FeCO_3$ layer corrosion product is more reactive than a polished iron to immobilize Se(IV) and Se(VI). The reacted iron surfaces were analysed by scanning electron microscopy (SEM) and energy dispersive spectrometer (EDS), X-ray diffraction (XRD), Raman spectrometry and micro-X-ray Absorption Spectroscopy (XAS). The result show that Se(IV) and Se(VI) were reduced and precipitated. The dominating phase was found to be $FeSe_2$.

Keywords Reductive immobilization · Selenium · Iron canister · Nuclear waste · Repository

D. Cui (✉)
Studsvik Nuclear AB, 61182 Nykoping, Sweden
e-mail: daqing.cui@studsvik.se

D. Cui
Department of Physical, Inorganic and Structural Chemistry, Stockholm University, 10691 Stockholm, Sweden

A. Puranen
Department of Chemistry, Royal Institute of Technology, 10044 Stockholm, Sweden

J. Devoy
IRSN/DPAM/SERCI/LE2C, 13115 Saint Paul-lez-Durance Cedex, France

A. Scheidegger
Paul Scherrer Institut, 5232 Villigen PSI, Switzerland

O. X. Leupin · P. Wersin
NAGRA, Hardstrasse 73, 5430 Wettingen, Switzerland

R. Gens
ONDRAF/NIRAS, 1210 Bruxelles, Belgium

K. Spahiu
SKB, 10240 Stockholm, Sweden

Introduction

For safety assessments for nuclear waste repositories, it is conservatively assumed that groundwater will enter through the engineered barrier system within a timeframe of >1,000 years [1]. After the canister have breached radionuclides will released from spent fuel and vitrified nuclear waste into groundwater. Among them, the fission product ^{79}Se ($t_{1/2} = 2.95 \times 10^5$ years) is one of important dose contributors due to its long half-life and high mobility of its oxidized anions SeO_3^{2-} and SeO_4^{2-}. Se(VI), Se(IV), Se(0) and Se(−I) (as $FeSe_2$) are more commonly observed in nature than Se(−II) (as FeSe). Se(0) and $FeSe_2$ are stable, poorly soluble and relatively resistant to re-oxidation [2]. Fe(II) and Fe(0) mediated redox reactions of Se, and the rate limiting steps have been examined using in situ X-ray absorption near-edge structure (XANES) [3]. It was shown that the reduction of Se(VI) in the presence of $Fe(II)_{aq}$ occurs in two steps, with rapid initial adsorption and conversion of Se(VI) to Se(IV) followed by a slow reduction of Se(IV) to Se(0). The rate of this reaction depends on both $Fe(II)_{aq}$ concentration and pH. At pH > 5, Fe(II) and Fe(III) precipitate as minerals such as green rust ($Fe_4^{II}Fe_2^{III}(OH)_{12}CO_3$), which can be more reductive than $Fe(II)_{aq}$ [4]. Se(VI) in a solution containing Cl^-, SO_4^{2-}, NO_3^-, HCO_3^-, and PO_4^{3-} in a capped vessel was found to be rapidly reduced by Fe(0) to Se(−II) [5]. In another investigation [6], a rapid

removal of Se(VI) from agricultural drainage water by Fe(0) was explained by two parallel mechanisms: (a) the reduction of Se(VI) to Se(IV), followed by rapid adsorption of Se(IV) to Fe-OH (iron oxyhydroxides) and (b) the adsorption of Se(VI) directly to Fe-OH followed by its reduction to Se(IV). During these two investigations [5, 6], the anoxic conditions were apparently not well controlled (Eh +400 to +500 mV, pH around 8) and the decrease of Se(VI) concentration might have been caused mainly by sorption on the large surfaces of iron oxide on corroded iron powder.

In the different deep repository concepts [7–10], iron metal will be used as canister material or as reinforcement material. Under anoxic deep groundwater conditions, iron is corroded by water to produce hydrogen gas and magnetite (Fe_3O_4) and/or Fe(II)–Fe(III)-hydroxides. Due to the reducing capacity of metallic iron and reducing and sorption capacities of iron corrosion products, metallic iron has been used to remove uranium [11] and other heavy metals [12, 13] from contaminated groundwater. A study on iron metal insert in contact with U(VI) containing synthetic groundwater has demonstrated that after a reaction time of 3 months an uneven few micron thick layer of carbonate green rust $\left(Fe_4^{II}Fe_2^{III}(OH)_{12}CO_3\right)$ with some micrometer sized UO_2 crystals are formed on iron surface [14]. Iron green rusts are characterized by a layered structure made of brucite-like sheets, positively charged due to Fe^{3+} cations [15, 16]. The sequence of iron corrosion is Fe(0) → $FeCO_3$ (siderite) → $\left(Fe_4^{II}Fe_2^{III}(OH)_{12}CO_3\right)$ (green rust) → Fe_3O_4 (magnetite) → Fe_2O_3 (hematite).

In the present work, the rates of the redox reactions between iron and dissolved fission product ^{79}Se, Se(IV) and Se(VI), and the speciation of the immobilized Se on iron surface under anaerobic groundwater conditions have been investigated.

Experimental

Iron surfaces

The 2 cm^2 sized iron coupons with 99.995% purity were polished by using up to #4000 sand-paper and rinsed with acetone, shortly before the batch experiments and stored and transported in an argon filled desiccator.

In a glass vessel, 200 mL 10 mM NaCl and 20 mM $NaHCO_3$ solution was first flushed with a gas mixture 99.7% Ar + 0.3% CO_2 for 3 days, then, polished iron coupons were added in the vessel. The pre-corrosion process was conducted for 2.5 years under flushing the same gas mixture. The corrosion products scrapped off from the corroded surface was analyzed by XRD using a Guinier camera with Cu $K_{\alpha 1}$ radiation (wavelength 1.5406 Å). Siderite ($FeCO_3$) and a minor fraction of magnetite (Fe_3O_4) were identified. The corroded iron surface was analyzed by Raman spectrometry, as shown in Fig. 1. The peak position at 1,079 cm^{-1} in Raman spectrum and XRD results clearly proved that the dominant corrosion product on the pre-corroded iron coupons is $FeCO_3$.

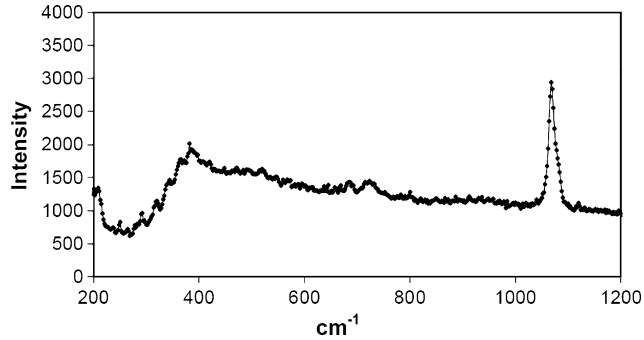

Fig. 1 Raman spectroscopic analysis of the corroded iron coupon reacted in the deoxygenated solution (10 mM NaCl + 20 mM $NaHCO_3$) for 2.5 years. The peak position at 1,079 cm^{-1} in the Raman spectrum matches well with that of $FeCO_3$

Solutions

A quantity of 1,000 μg/g selenate Se(IV) and selenite Se(VI) stock solutions were made by adding relevant chemicals with analytical grade purity into a solution containing 10 mM NaCl and 2 mM $NaHCO_3$, the pH values of the solutions were adjusted to 8.2.

Arrangement and procedures

All batch experiments as described in Table 1 were conducted in glass reaction bottles in an atmosphere controlled vessel. To evaluate the influence of CO_2 partial pressure on the pH shift of the solution caused by iron oxidation, Ar is used in Exp 2 and 3 and Ar + 0.03% CO_2 mixture used in all other experiments as purging gases. To test the role of corrosion layer of iron coupon on the Se immobilization, the iron coupons used in Exp 3, 5 and 7 were pre-corroded for 2.5 years with $FeCO_3$ as the major corrosion product.

An in situ oxygen trap with $FeCO_3$ as O_2 consumer and $CaCO_3$ as a pH buffer, described previously [14], was used. After 5 days of flushing with the gas mixture, iron coupons were added into the reaction bottles with 20 mL solutions. Thereafter, 0.2 mL solution samples were taken during the experiment and analyzed by inductively coupled plasma mass spectrometry (ICP-MS). After the experiments, some corrosion products on the iron coupons were scrapped off under Ar atmosphere, and immediately analyzed by XRD as described in "Iron surfaces" above.

Table 1 Se(IV)/Se(VI) experiments, the effects of corrosion layer

Exp no.	Solid properties	Ionic medium	CO_2% in Ar	Exp. time (day)	Initial Se speciation and conc. (ng/g)	Final Se (ng/g)	pH initial	pH final	XRD SEM-EDS XAS
1	Polished Fe(0)	10 mM NaCl 2 mM $NaHCO_3$	0.03	56	Se(IV) 5000	<DL[a]	8.2	8.0	Yes
2	Polished Fe(0)	10 mM NaCl 2 mM $NaHCO_3$	0	1st, 3 2nd, 6	Se(IV) 1st, 1493 2nd, 7890	<DL[a] 2500	8.20	6.27	Yes
3	Corroded 2.5 year $FeCO_3$	10 mM NaCl 2 mM $NaHCO_3$	0	1st, 3 2nd, 6	Se(IV) 1st, 1493 2nd, 7890	<DL[a] 250	8.20	6.23	No
4	(a) Polished (b) $FeCO_3$ corr.	10 mM NaCl 2 mM $NaHCO_3$	0.03	60	Se(VI) (a) (b) 10130	(a) 8600 (b) 7950	8.2	Not measured	Yes
5	(a) Polished (b) $FeCO_3$ corr.	10 mM NaCl 2 mM $NaHCO_3$ 5 μg/g U(VI)	0.03	22	Se(VI) (a) (b) 5310	(a) 4400 (b) 3000	8.2	Not measured	Yes

[a] <DL below detection limit, 50 ng/g

The remaining part of the iron coupon was embedded in epoxy resin, polished for SEM, EDS, μ-XAS and μ-X-ray fluorescence (XRF) analysis. μ-XRF and Se K-edge (12.6 keV) μ-XAS experiments on the iron coupon with immobilized Se were performed at the ALS beamline 10.3.2, a bending magnet beamline dedicated to μ-XAS. The measurements were conducted using Si(111) monochromator crystals, a pre-focusing mirror and a pair of Kirpartrick-Beaz (KB) mirrors. The beam size at the sample position was $\sim$5 μm × 5 μm.

Results and discussion

Se(IV) immobilization on iron surface

In Exp 1, as described in the Table 1, Se(IV) concentrations in the solution dropped from 5 μg/g (6.5×10^{-5} M) to 2.5 μg/g within 2 days and to below 1 μg/g after 10 days.

In the Exp 2 and 3 conducted in a solution purged with Ar, iron reacts with H_2O molecular, oxidative species or OH^- and therefore pH of the solution decreased. After the first experimental period of 3 days, Se concentrations decreased to a level below the detection limit (50 ng/g). In the second experiment period, 6 days after of adding 7.9 μg/g Se(IV), Se(IV) concentrations dropped to 2,500 ng/g and 250 ng/g, respectively. In other experiments (Exp 1, 4, 5, 6, 7), the solutions were equilibrated with Ar + 0.03% CO_2 atmosphere, therefore, the pH drops were not significant due to the pH buffering capacity of $NaHCO_3$–CO_2 system. The results of experiments with Se(IV) and polished or corroded iron coupons can be summarized as (a) Se(IV) immobilization on iron surface is a fast process and (b) after forming $FeCO_3$ layer on a iron surface, Se(IV) immobilization process on the corroded iron is enhanced.

Se(VI) concentration drops in the Exp 4a and b indicates that the immobilization of Se(VI) on iron surface is much slower than that of Se(IV) under the same conditions. The pre-corroded iron coupon reacts with Se(VI) slightly faster than the polished one. Comparing Se(VI) concentration drops in Exp 4–5 and Exp 6–7, one can see that after adding 5 μg/g U(VI) in the solution, the Se(VI) immobilization can become much faster. This finding is important because all high level radioactive wastes, either spent nuclear fuel or glass wastes, contain much more uranium than selenium. It can be explained that carbonate green rust, that formed on iron surface in U(VI) solution [14], can enhance Se(VI) (as SeO_4^{2-}) immobilization.

After Exp 1, pH and Eh values of the solution were measured using pre-calibrated electrodes, pH was 8.5 and Eh ranged between −247 and −255 mV (vs. SHE). Comparing with other published work [5, 6] (Eh around +500 mV, pH = 8), the air contamination in this work was neglectable.

After Exp 1 and 2, the corrosion products formed on the iron coupons were quickly scrapped off and analyzed by XRD. Distances d(Å) and intensity values of the diffraction peaks for the dark-green blue colored corrosion product match well with the reported for iron carbonate hydroxide, also called carbonate green rust, $\left(Fe_4^{II}Fe_2^{III}(OH)_{12}CO_3\right)$, (JCPDS number 46-0098) [14, 15]. No other iron or Se

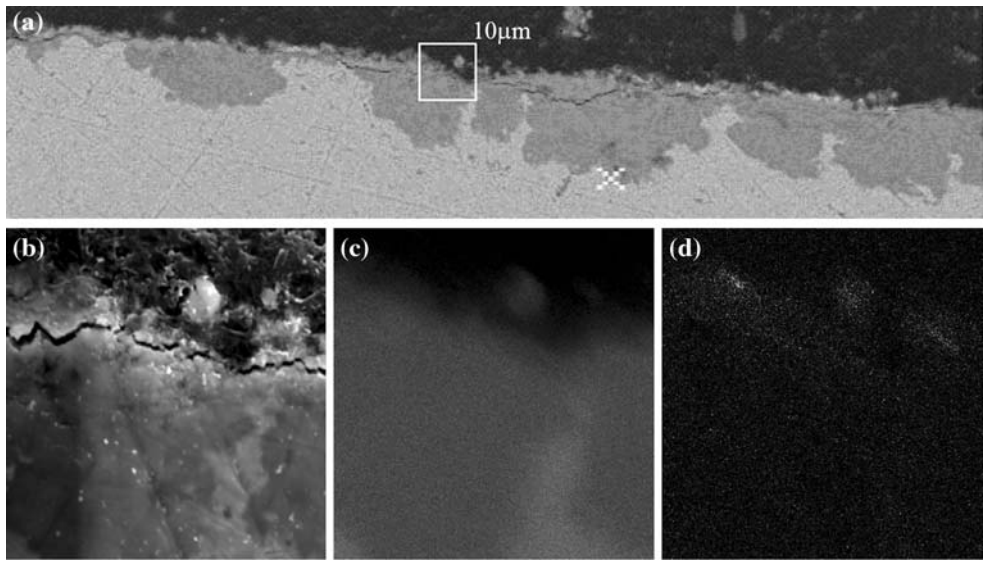

Fig. 2 SEM images (**a**) and (**b**) and EDS element mapping, (**c**) for Fe and (**d**) for Se, of the cross section of corrosion layer on a pre-corroded iron coupon ($FeCO_3$ coated) reacted in Exp 3, Table 1. The 10 μm sized *square* marked in (**a**) represents the size and location of (**b**), (**c**) and (**d**). The *upper black part* of (**a**) is epoxy and *lower light grey part* of (**a**) is iron matrix, the *darker grey parts* are uneven iron corrosion product ($FeCO_3$). Two to three percent Se "hot" spots are found on outer layer of iron

phases were found by XRD method in the corrosion products.

The SEM-EDS analysis of the cross section of iron coupon reacted in Exp 3, as shown in Fig. 2, indicates that an uneven 5–15 μm thick grey coloured corrosion product (proved to be $FeCO_3$ by Raman spectroscopy and XRD) was formed on the iron coupon after 2.5 years pre-corrosion under anaerobic conditions. Selenium is not evenly distributed over the corrosion layer, but enriched in some spots. Some of them containing 2–3% Se were observed on the outer layer of corrosion products, as shown in Fig. 2d).

Figure 3 shows a μ-XRF map of Fe and Se (at 13 keV) of a cross section of the surface of Fe coupon interacted in Exp 1. The iron surface exposed to an anaerobic Se(IV) solution is facing down in the image. An uneven iron

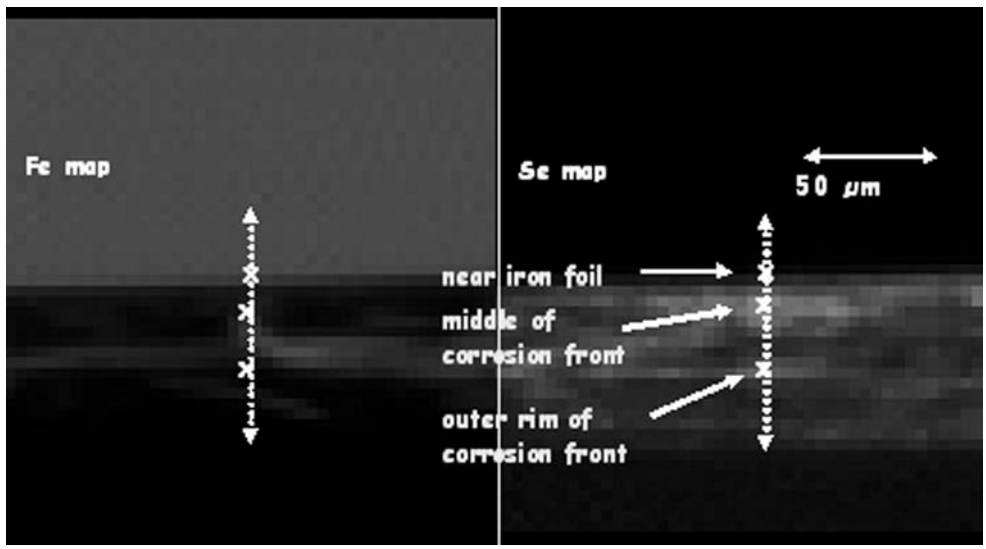

Fig. 3 μ-XRF mapping of Fe and Se of a horizontally cross section of enlarged corrosion layer of the iron coupon interacted in Exp 1. Fe and epoxy are represented in *grey* and *black*, respectively (*left*), and Se in *white* (*right*)

corrosion layer with heterogeneous Se distribution was observed. Very porous corrosion product observed in XRF Fe mapping in Fig. 3 (left) corresponds the cotton like dark-green colored corrosion product that attached on the corroded iron surface observed visually through the glass vessel wall during Exp 1 and 2 and a previous work [14]. It is proved to be the carbonate green rust by XRD analysis. The XRF Se mapping given in Fig. 3 (right) indicates the heterogeneous Se distribution in the porous and softly attached corrosion layer (green rust) on the iron coupons.

The results of XANES analysis on immobilized Se(IV) (Exp 1) and Se(VI) (Exp 5b) in corrosion layer of iron coupons are shown in Fig. 4. XANES spectra of Se(IV) immobilized at different depth of iron corrosion product are given in Fig. 4 (upper). The peak positions and intensities of XANES spectra suggest that the selenium immobilized at middle depth of the iron corrosion layer is better crystallized.

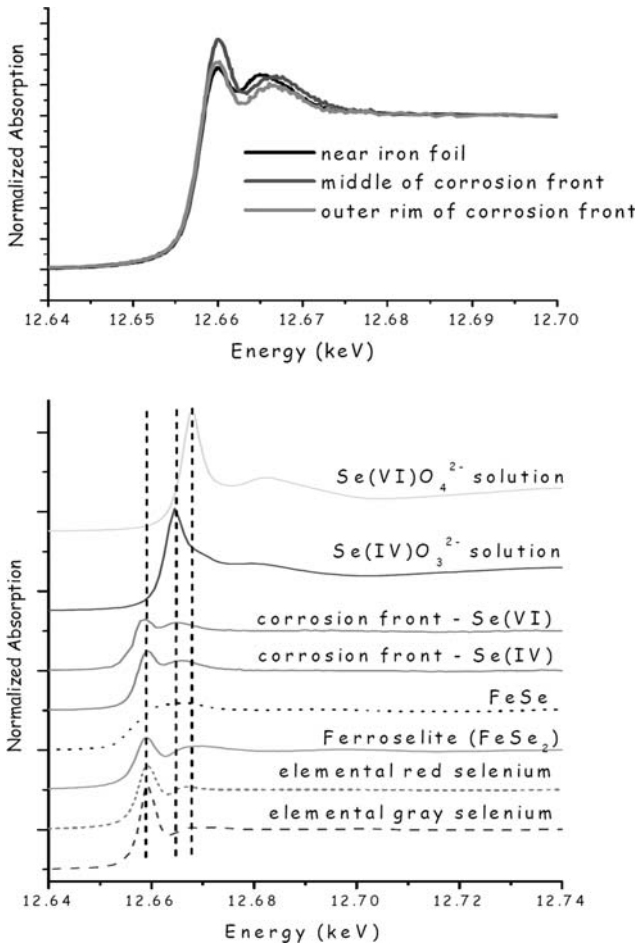

Fig. 4 XANES spectra, *upper*: that collected along a vertical line scan from the outer side of the sample through the corrosion layer into the iron coupon, as cross marked in Fig. 3, in a colour sequence; *lower*: XANES of several materials and the corrosion fronts on the samples from the experiments with Se(IV) (Exp 1) and Se(VI) (Exp 5b) as initial Se oxidation states

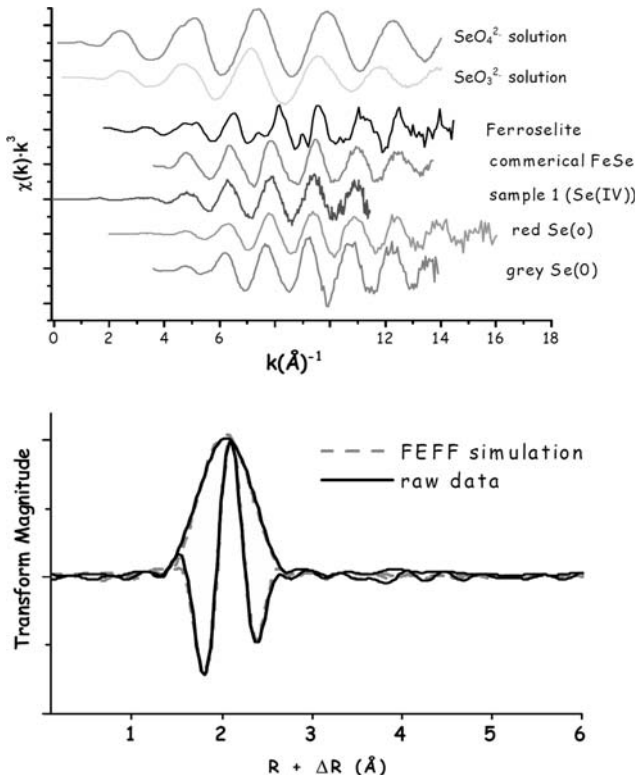

Fig. 5 Se K-edge EXAFS, *upper*: Se-rich hot spot within green rust corrosion layer from Exp 1 and some reference materials and *lower*: with Se–Fe backscattering contribution (peaks at ~2.41 Å) and transform magnitude

XANES spectra given in Fig. 4 (lower) reveals that (a) Se(0) and Se (−I) (as $FeSe_2$) display very similar XANES spectra and (b) both Se(IV) (Exp 1) and Se(VI) (Exp 5b) were reduced and immobilized on iron surface as Se(0) and/or $FeSe_2$.

The results of EXAFS measurements at Se rich spots on the green rust on the sample from Exp 1 and several reference materials are presented in Fig. 5. The EXAFS spectra shown in Fig. 5 (upper) were best fit using a Se–Fe backscattering contribution at ~2.41 Å. While this bond distance is much longer than the initial Se–O distances in $Se(IV)O_3^{2-}$ (~1.70 Å) and is well in agreement with Fe–Se distances in $FeSe_2$ minerals described in the literature (Ferroselite: 2.35 and 2.385 Å; Dzharkenite: 2.42 Å). This finding suggests that Se(IV) did undergo a reduction process within a time frame of <2 months and that selenium is coordinated within the green rust layer as Se(−I), as a form with similar Fe–Se band distance as that of $FeSe_2$. The reductive immobilization of Se(VI) by iron surface has been proved by XAS method, but to verity which oxidation states, Se(0) or Se(−I), is dominant in the immobilized

selenium on iron surface, further EXAFS work need to be conducted.

Summary

- The results of ICP-MS analysis on Se concentration drops and XRD, SEM-EDS and XAS analysis on the corroded iron surface show that under anoxic environments both Se(IV) and Se(VI) can be reductively immobilized as Se(0) and/or $FeSe_2$ by iron canister surface. After the Se immobilization, carbonate green rust was observed as the dominant iron corrosion product on the iron surface.
- Se(IV) can be reductively immobilized by metallic iron much faster than Se(VI).
- The pre-corroded iron surfaces (with $FeCO_3$) can reduce and immobilize Se(IV) and Se(VI) much faster than that with polished iron surfaces.
- μ mole level U(VI) in the solution can enhance the Se(VI) immobilization process on iron surfaces.
- EXAFS result confirmed that Se(IV) in groundwater can be reduced by iron and/or iron corrosion products ($FeCO_3$ and green rust) to a insoluble Se(−I) phase, as $FeSe_2$.

Acknowledgements This work has been supported and coordinated mainly by Swedish Nuclear Fuel and Waste Management Co. (SKB), Sweden, and partly by NAGRA, Switzerland, ONDRAF/NAIRAS, Belgium and sixth FP NF_PRO WP2.5.7, European Commission. The contributions of M. Granfors, J. Low and R. Lundström on the sample analysis are gratefully acknowledged.

References

1. KBS-3 (1983) Final storage of spend nuclear fuel. Report by the Swedish Nuclear Fuel Supply Co., Stockholm, Sweden
2. Noland WE (ed) (2005) Book: chemical thermodynamics of selenium 7. ISBN: 0-444-51403-1, imprint Elsevier, p 894
3. Myneni SCB, Tokunaga TK, Brown GE (1997) Science 278:1106
4. Cui D, Eriksen T (1996) Environ Sci Technol 30:2259
5. Zhang Y, Amrhein C, Frankenberger W (2005) Sci Total Environ 350:1–11
6. Zhang Y, Wang J, Amrhein C, Frankenberger WT (2005) J Environ Qual 34:487
7. SKB (1999) SR 97—post closure safety. Main report, vols I, II. SKB technical report TR-99-06, Stockholm, Sweden
8. SKB (2006) Long term safety for KBS-3 repositories at Forsmark and Laxemar—a first evaluation. SKB technical report TR-06-09, October 2006
9. Johnson LH, Smith PA (2000) The interaction of radiolysis products and canister corrosion products and the implications for radionuclide transport in the near field of a repository for spent fuel. Nagra technical report NTB 00-04, Switzerland
10. Craeye B, De Schutter G, Bel J, Van Humbeeck H, Van Gotthem A (2007) Development of a SCC composition fro disposal of heat-emitting radioactive waste in Belgium. In: 5th Intern, RILEM symposium on self compacting concrete, 3–5 Sep 2007
11. Gu B, Liang L, Dickey J, Dai S (1998) J Environ Sci Technol 32:3366
12. Loyaux-Lawniczak S, Refait P, Lecomte P, Ehrhardt J-J, Genin J-MR (1999) Hydrol Earth Syst Sci 3:593
13. Loyaux-Lawniczak S, Refait P, Lecomte P, Ehrhardt J-J, Genin J-MR (2000) Environ Sci Technol 34:438
14. Cui D, Spahiu K (2002) Radiochim Acta 90:623
15. Hansen HCB (1989) Clay Mineral 24:663
16. Hansen HCB (2002) Environmental chemistry of iron(II)-iron(III) LDHs (green rusts). In: Rives V (ed) Layered double hydroxides: present and future. Nova Science Publishers, NY, p 413